Nucleic Acids Research, 1998, Vol. 26, No. 3 735–743

Determination of interactions between structured nucleic acids by fluorescence resonance energy transfer (FRET): selection of target sites for functional nucleic acids

Naruhisa Ota[1,2,3], Ken′ichi Hirano[4], Masaki Warashina[1,3], Alex Andrus[5], Bashar Mullah[5], Kenichi Hatanaka[2] and Kazunari Taira[1,3,*]

[1]National Institute for Advanced Interdisciplinary Research, and National Institute of Bioscience and Human Technology, Agency of Industrial Science & Technology, MITI, Tsukuba Science City 305, Japan, [2]Department of Bioscience and Biotechnology, Tokyo Institute of Technology, Nagatsuta-cho 4259, Midori-ku, Yokohama 226, Japan, [3]Institute of Applied Biochemistry, University of Tsukuba, Tsukuba Science City 305, Japan, [4]Tsukuba Research Laboratory, Hamamatsu Photonics K. K., Tokodai 5-9-2, Tsukuba Science City 300-26, Japan and [5]Applied Biosystems, Division of Perkin Elmer Co., Foster City, CA 94404, USA

Received October 28, 1997; Accepted December 11, 1997

ABSTRACT

We previously developed a method for monitoring the integrity of oligonucleotides *in vitro* and *in vivo* by quantitating fluorescence resonance energy transfer (FRET) between two different fluorochromes attached to a single oligonucleotide. As an extension of this analysis, we examined changes in the extent of FRET in the presence or absence of target nucleic acids with a specific sequence and a higher-ordered structure. In this system FRET was maximal when probes were free in solution and a decrease in FRET was evidence of successful hybridization. We used a single-stranded oligodeoxyribonucleotide labeled at its 5′-end and its 3′-end with 6-carboxyfluorescein and 6-carboxytetramethylrhodamine, respectively. Incubation of the probe with a single-stranded complementary oligonucleotide reduced the FRET. Moreover, a small change in FRET was also observed when the probe was incubated with an oligonucleotide in which the target site had been embedded in a stable hairpin structure. The decrease in the extent of FRET depended on the length of the stem region of the hairpin structure and also on the higher-ordered structure of the probe. These results indicate that this spectrofluorometric method and FRET probes can be used to estimate the efficacy of hybridization between a probe and its target site within highly ordered structures. This conclusion based on changes in FRET was confirmed by gel-shift assays.

INTRODUCTION

Attempts at the artificial regulation of gene expression have been made for the development of therapies for diseases such as cancer and AIDS. As one strategy for such therapy, the intracellular injection of an antisense oligonucleotide or ribozyme has been proposed (1–4). Such oligonucleotides can inhibit the synthesis of target proteins by annealing to the corresponding mRNA, transcribed from the target gene, with subsequent degradation of the mRNA (5–7). Functional oligonucleotides of this type have the potential to serve as therapeutic agents in humans, without side effects, so long as natural backbones are used, because of their high specificity, which depends on the formation of a duplex with the complementary mRNA. To exploit this approach, it is important to select an appropriate target site within the RNA. If a designed oligonucleotide is unable to anneal at the selected site within the target RNA, which has a highly ordered structure, gene expression will not be inhibited. The annealing efficiency of oligonucleotides of their target sites is known to be affected by the highly ordered structure of RNA molecules in solution and in cells. In general, single-stranded regions, such as those in loop structures, are suitable for hybridization to functional oligonucleotides (1,2,8,9). In this report, we present a convenient method for examining whether a designed oligonucleotide can hybridize efficiently to its target by monitoring fluorescence resonance energy transfer (FRET).

FRET is an interesting fluorescence-related phenomenon (10,11). When the fluorescence spectrum of one fluorophore (the donor) overlaps with the excitation spectrum of another fluorophore (the acceptor), the excitation of the donor induces fluorescence of the acceptor, while its own fluorescence decreases (Fig. 1). The extent of FRET is extremely sensitive to the distance between the donor and the acceptor, being inversely proportional to the sixth power of the distance. This phenomenon can be exploited to study intermolecular and intramolecular relationships in biophysical systems and cell biology. Various studies of nucleic acids involving FRET have been reported, with emphasis for example, on structural analysis (12–17), oligonucleotide hybridization (18–21), nucleotide degradation (22–24), the polymerase chain

*To whom correspondence should be addressed at: Institute of Applied Biochemistry, University of Tsukuba, 1-1-1 Tennoudai, Tsukuba Science City 305, Japan. Tel/Fax: +81 298 53 4623; Email: taira@nibh.go.jp

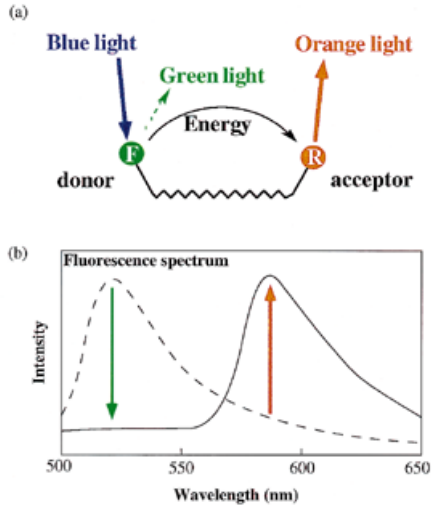

Figure 1. Fluorescence resonance energy transfer. (**a**) When the fluorescence spectrum of one fluorophore (donor; F) overlaps with the excitation spectrum of the other fluorophore (acceptor; R), the excitation of the donor induces the emission of fluorescence from the acceptor, while its own fluorescence decreases. (**b**) In this study, 6-carboxyfluorescein and 6-carboxytetramethylrhodamine were employed as the donor and the acceptor, respectively. When fluorescence resonance energy transfer (FRET) takes place, the excitation of 6-carboxy-fluorescein by blue light (492 nm) results in the emission of orange light (586.5 nm) from 6-carboxytetramethylrhodamine, while the emission of green light (519 nm) from 6-carboxyfluorescein decreases.

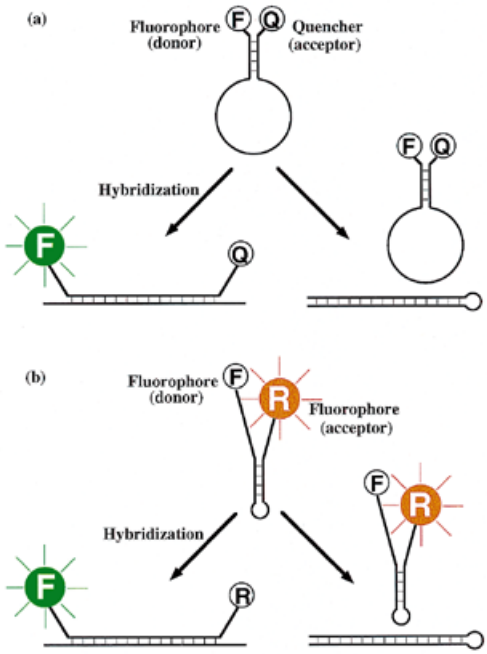

Figure 2. Detection of hybridization by the use of molecular beacons and by our probes. (**a**) Labeled oligonucleotides with a fluorophore as a donor (F) and a quencher (Q) as an acceptor can be used to identify the presence of a complementary sequence in solution (27). Successful hybridization of the molecular beacon with the target results in emission from the donor. (**b**) Monitoring of the integrity of oligonucleotides *in vitro* and *in vivo* is possible by exploiting the FRET between two different fluorochromes attached to a single oligonucleotide (22), which can also be used to detect hybridization. Our probe used in this study (Fig. 1a) in a single-stranded form is detectable as a result of emission from the acceptor (R) that could be excited directly by an appropriate light source or by transfer of energy from the donor. In the case of molecular beacons, probes are dark when free in solution but they fluoresce brightly when hybridized to targets. In the case of our probes, the extent of FRET is maximal when probes are free in solution and a decrease in FRET indicates successful hybridization.

reaction (25–29), and the release of oligonucleotides from liposomes (30).

Most FRET studies with nucleic acids have involved oligonucleotides with single end-labels, with a few exceptions (12,19,22,25–29). An oligonucleotide that has been labeled with a donor and an acceptor dye at each end would be a suitable probe for detection of hybridization (Fig. 2). Tyagi and Kramer (27) measured the extent of FRET between a fluorophore as a donor and a quencher as an acceptor bound to a single oligonucleotide ('molecular beacons') to detect the presence of complementary sequences in solutions (Fig. 2a). We independently developed a method for monitoring the integrity of oligonucleotides *in vitro* and *in vivo* by exploiting FRET between two different fluorochromes attached to a single oligonucleotide (Fig. 1; ref. 22), which can also be used to detect hybridization (Fig. 2b). Although molecular beacons are suitable for measurements of hybridization *in vitro*, the localization of the intact probe cannot be investigated in living cells because of the use of a quencher as an energy acceptor that emits no fluorescence. As an extension of our first FRET study (22), we examined the feasibility of using a fluorescently double-labeled oligonucleotide (Fig. 2b) to examine whether a specific sequence within a highly ordered target structure might be accessible to a probe. In this case, fluorescently double-labeled intact and functional nucleic acids, such as antisense DNA or RNA and ribozymes, should be detectable in living cells (22). To examine the potential applicability of such FRET probes to studies *in vivo*, we labeled an oligonucleotide with 6-carboxytetramethylrhodamine as the fluorescent acceptor and with 6-carboxyfluorescein as the fluorescent donor. This probe, in single-stranded form, is detectable as a result of emission from the acceptor when it is excited directly with an appropriate light source or by energy transfer from the donor.

Since there have been no reports about the efficacy of FRET when both the probe and the target molecule have highly ordered structures, we synthesized several targets of different lengths and analyzed the correlation between the FRET and the extent of hybridization between the probe and the target. Specifically, we analyzed spectrofluorometrically the FRET of the probe after incubation with various oligodeoxyribonucleotides, which should adopt single-stranded or hairpin structures under the hybridization conditions. We demonstrate in this report that measurements of FRET using fluorescently double-labeled oligonucleotides are useful for the selection of efficient target sites for functional oligonucleotides, such as antisense DNA and RNA, ribozymes and DNA enzymes. Moreover, fluorescently double-labeled oligonucleotides are useful for the fluorometric detection of hybridized bands in gel-shift assays. Our results suggest that a high-throughput, fluorescence-based assay could be constructed to screen for optimal mRNA or genomic DNA antisense targets.

MATERIALS AND METHODS

Synthesis of the probe (F-D32-R)

All oligonucleotides were synthesized on a DNA/RNA Synthesizer (ABI 394; Perkin-Elmer, CA) by phosphoramidite chemistry (31) with a set of A^{bz}, G^{dmf}, C^{bz} and T phosphoramidite nucleosides. Reagents were obtained from the manufacturer (PE Applied Biosystems). Syntheses of unlabelled oligonucleotides were

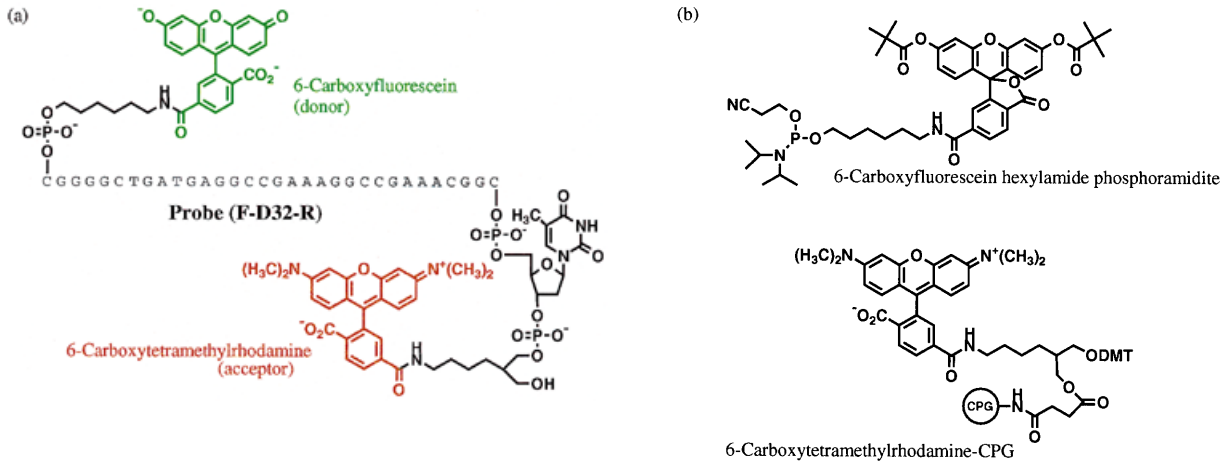

Figure 3. Structures of the probe (**a**) and reagents (**b**) for the synthesis of the probe (F-D32-R). The 32mer deoxyribonucleotide probe F-D32-R was modified with two fluorophores, namely 5′-6-carboxyfluorescein and 3′-6-carboxytetramethylrhodamine.

conducted on the 0.2 µmol scale on 1000 Å controlled-pore-glass support (CPG) with the 0.2 µM cyanoethyl (CE) synthesis cycle and the CESS cleavage end procedure. The double-labeled probe, F-D32-R, was synthesized on the 1 µmol scale on a 6-carboxytetramethylrhodamine-CPG synthesis support (Fig. 3). Using the non-nucleosidic, 2-aminobutyl-1,3-propanediol backbone (32), we prepared the support by protection of hydroxyl groups with dimethoxytrityl (DMT) and of amino groups with Fmoc (9-fluorenylmethoxycarbonyl), with subsequent derivatization of the other hydroxyl moieties with succinic anhydride and coupling with 500 Å aminopropyl-CPG after dicyclohexylcarbodiimide (DCC)/HOBt activation. Deprotection of Fmoc by brief treatment with piperidine and coupling with 6-carboxytetramethylrhodamine-*N*-hydroxysuccinimide ester yielded the synthesis support, loaded at 32 µmol/g (DMT analysis at 490 nm, ε = 70 000; ref. 33). The 6-carboxytetramethylrhodamine-CPG synthesis support was used in the synthesis of F-D32-R on the 1-µmole scale with the same reagents and the same synthesis cycle as the unlabelled oligonucleotides. The 5′ terminus was labeled with 6-carboxyfluorescein hexylamide phosphoramidite (Fig. 3), with >90% coupling efficiency, using a 120 s coupling wait step (34). Since 6-carboxytetramethylrhodamine is sensitive to ammonium hydroxide, cleavage from the CPG support and deprotection were performed with 2 ml of a mixture of tert-butylamine, water and methanol (1/2/1, v/v) for 90 min at 85°C (35). The dried crude sample was purified by reverse-phase HPLC (PLRP-1; Hamilton Co., Reno, NV). Two injections of ~100 OD (A_{260}) units each were made on a column (7 mm i.d. × 300 mm) at a flow rate of 1 ml/min, with detection at 260 nm and elution with a linear gradient of 5–40% B in A over 30 min (A, 3% acetonitrile in 0.1 M triethylammonium acetate; B, acetonitrile). The collected fractions were evaporated to dryness under a vacuum and products were precipitated in 3 vol of isopropanol after the residue had been dissolved in a minimum volume of 3 M sodium acetate to give 20 OD units (~600 µg) of F-D32-R. The absorbance spectrum had the expected peaks at 260, 491 and 560 nm.

Measurements of fluorescence

For hybridization to the 32mer complementary strand (ss–Target), the control strand (D32), the stem strand (hairpin–Target), duplex–Target or uncomplementary hairpin–Target, the probe (F-D32-R) was dissolved at 30 pmol/ml in a solution of 10 mM Tris–HCl (pH 7.4), 0.1 M NaCl, 5 mM $MgCl_2$ and 10 mM EDTA. For the hybridization of F-D32-R, the probe was dissolved at 30 pmol/ml in a solution of 50 mM Tris–HCl (pH 8) and 30 mM $MgCl_2$. The duplex–Target was generated by mixing 150 pmol of ss–Target with the same amount of D32, heating at 85°C for 5 min, and cooling slowly to room temperature. The oligonucleotides with stem structures (hairpin–Target, duplex–Target, uncomplementary hairpin–Target, and stem–Targets) were heated at 85°C for 5 min in solution and then solutions were cooled slowly to ambient temperature over 3 h before use. Before all measurements, solutions in cuvettes were vortexed to ensure homogeneity. The measurements of fluorescence were made in cuvettes with a 1 cm path length in a fluorescence spectrophotometer (model 850; Hitachi, Hitachi City, Japan) with excitation at 492 nm. All measurements were made in triplicate at 25°C.

Measurements of fluorescence anisotropy

The fluorescence of 6-carboxytetramethylrhodamine bound to the probe (F-D32-R; 30 nM) was measured in the hybridization buffer with the fluorescence spectrophotometer at 586.5 nm with excitation at 540 nm. Fluorescence anisotropy was calculated from fluorescence intensities as described in the literature provided by the manufacturer of Hitachi. Fluorescence anisotropy was obtained from the following equation:

$$r = (Ih - Iv)/(Ih + 2Iv) \quad \mathbf{1}$$

where Ih and Iv are the intensities of the fluorescence parallel and perpendicular to the direction of polarization of the excitation light, respectively.

Gel shift assays using a fluorescence imaging analyzer

For the confirmation of hybridization of the probe with ss–Target or hairpin–Target (Fig. 6), 10 pmol of F-D32-R was incubated with various amount of either ss–Target, D32, hairpin–Target, or uncomplementary hairpin–Target in a 20 µl solution that contained 10 mM Tris–HCl (pH 7.4), 0.1 M NaCl, 5 mM $MgCl_2$ and 10 mM EDTA. After 90 min incubation, the mixture was separated by a native 12% polyacrylamide gel electrophoresis and analyzed by a

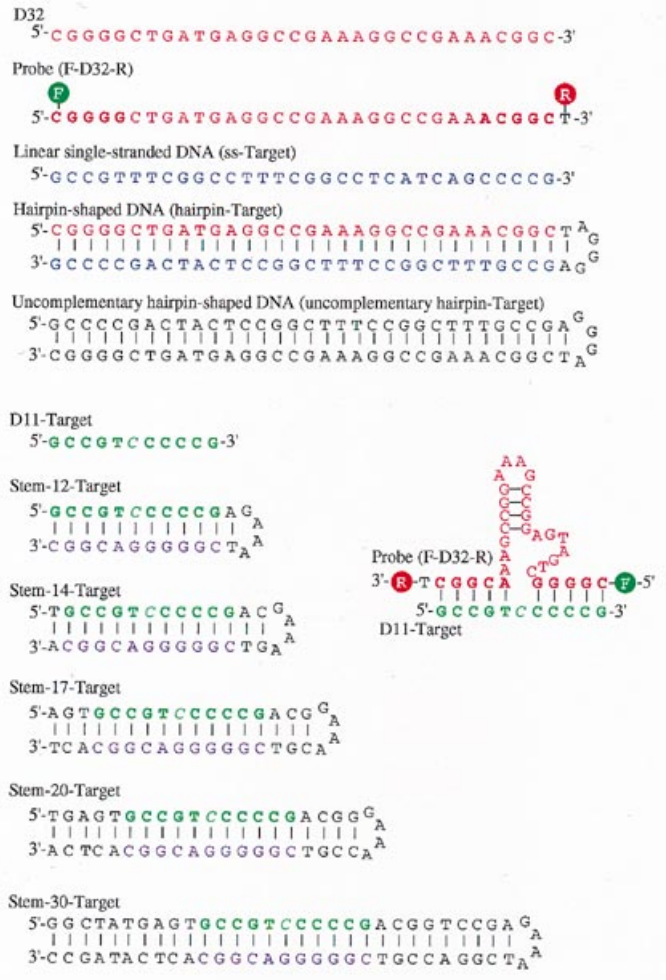

Figure 4. Sequences of the probe and the target molecules. The sequence of the probe corresponded to that of the 32mer hammerhead ribozyme (37–40). Nine target DNAs were used in this study. Linear single-stranded DNA (ss–Target), hairpin-shaped DNA (hairpin–Target), and hairpin-shaped DNA without complementary sequence (uncomplementary hairpin–Target) were used for investigations of the interactions between the non-structured probe and non-structured or structured targets. D11–Target and Stem-##–Targets were used for studies of hybridization between the structured probe and non-structured or structured targets. Bold letters indicate sites of hybridization with the probe. The secondary structure of the probe that hybridized to D11–Target is shown in the middle of the Figure on the right.

fluorescence image analyzer (model FluorImager 595; Molecular Dynamics, CA). For the affinity study (Fig. 10), 2 pmol of F-D32-R and 2 pmol of ss–Target were incubated with various amounts of D32 in 10 µl of the same solution described above. After an overnight incubation, the mixture was separated by a native 12% polyacrylamide gel electrophoresis, the fluorescence measured as described above and the quantitation made by ImageQuant (Molecular Dynamics, CA). The extent of complex formation was estimated by the following equation:

$$\text{Extent of complex formation (\%)} = (\text{Vol} - \text{Vol}_0)/(\text{Vol}_{100} - \text{Vol}_0) \times 100 \quad \mathbf{2}$$

where Vol is the level of fluorescence at the band of complex of F-D32-R with ss–Target, Vol_0 is that in the absence of neither ss–Target or D32, and Vol_{100} is that without D32.

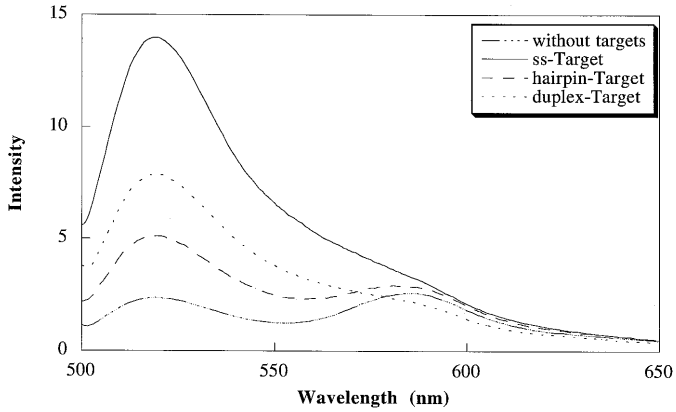

Figure 5. Typical fluorescence spectra of a solution, after a 70 min incubation, that contained 30 pmol of F-D32-R and either 150 pmol of ss–Target (solid line), or 150 pmol of hairpin–Target (broken line), or duplex–Target formed by the incubation of 150 pmol of ss–Target and the same amount of D32 (dashed line). The lowest line shows the fluorescence spectrum of the probe itself.

RESULTS AND DISCUSSION

A fluorescently double-labeled oligonucleotide probe with two fluorescent moieties and its target molecules

In order to examine the efficacy of FRET when either the probe or the target molecule has a highly ordered structure, we synthesized several kinds of such nucleic acid (Figs 3 and 4) and analyzed the correlation between the extent of FRET and the degree of hybridization among the structured molecules. The sequence of the control DNA, designated D32, corresponded to that of the 32mer hammerhead ribozyme, R32, which is used extensively in our laboratory (36–41). The probe, designated F-D32-R, was synthesized by modification of the D32 oligodeoxyribonucleotide with 6-carboxyfluorescein as the donor and 6-carboxytetramethylrhodamine as the acceptor at its 5′-end and 3′-end, respectively (Fig. 3; see also Materials and Methods). For use as target molecules, we synthesized eight kinds of either non-structured or hairpin-shaped DNA, as shown in Figure 4.

The emission spectrum of the fluorescent oligonucleotide F-D32-R was measured in the buffered solution that was to be used in hybridization experiments [10 mM Tris–HCl (pH 7.4), 0.1 M NaCl, 5 mM $MgCl_2$ and 10 mM EDTA]. The buffered solution itself gave no detectable signal above background. The solution that contained the probe had peaks of fluorescence, at 519 and 586.5 nm, when excited at 492 nm (the lowest spectrum in Fig. 5). These wavelengths corresponded to the peaks of fluorescence emitted by 6-carboxyfluorescein and 6-carboxytetramethylrhodamine, respectively. The weak intensity of fluorescence of the donor and relatively strong intensity of fluorescence of the acceptor indicate that the energy was transferred from the excited donor to the unexcited acceptor and, thus, that this modified oligonucleotide was suitable as a FRET probe.

Interaction between the probe (F-D32-R) and either linear complementary DNA (ss–Target) or hairpin-shaped DNA (hairpin–Target)

To determine whether the double-labeled probe, F-D32-R, might be useful to examine interactions with highly ordered target molecules,

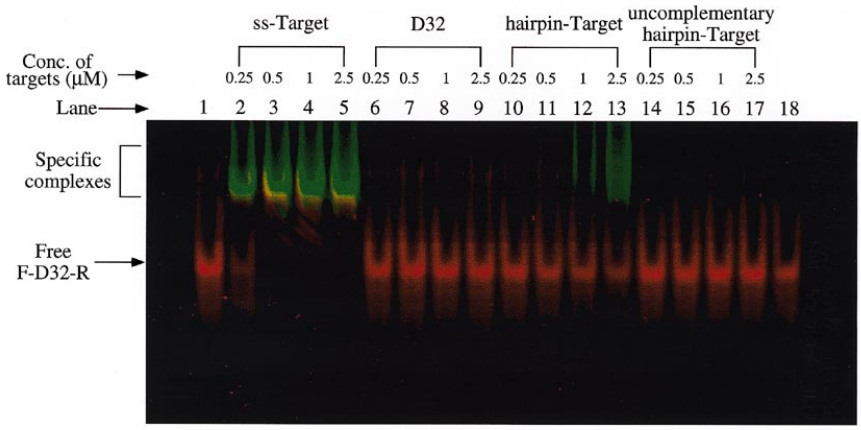

Figure 6. Typical gel image of gel-shift assays analyzed by a fluorescence imaging analyzer. In the solution containing 10 mM Tris–HCl (pH 7.4), 0.1 M NaCl, 5 mM $MgCl_2$, and 10 mM EDTA, 400 nM of the probe and none (lanes 1 and 18), 250 nM (lanes 2, 6, 10 and 14), 500 nM (lanes 3, 7, 11 and 15), 1000 nM (lanes 4, 8, 12 and 16) and 2500 nM (lanes 5, 9, 13 and 17) of each target were incubated for 70 min and followed by a 12% native PAGE. Resultant gels were analyzed by a fluorescence imaging analyzer and the level of fluorescence at 530 nm and that at 590 nm were calculated by a computer program (FluorSep, Molecular Dynamics, CA). The green and red bands indicate the fluoresence at 530 and 590 nm, respectively. The decrease in the extent of FRET (red color) is accompanied by the increase in the shifted band (green color).

we used three types of oligodeoxyribonucleotide as model targets for the probe. The first target was a 32mer single-stranded linear DNA (ss–Target) with a sequence complementary to that of the probe. The second type, a 70mer, consisted of the sequence of the probe itself and the sequence of ss–Target, with a four base loop. This target was designated hairpin–Target (Fig. 4). In the latter case, the target site for the F-D32-R is not available unless the intramolecular duplex is disrupted by intermolecular interaction with the F-D32-R. The sequence of the third type (uncomplementary hairpin–Target) was in the reverse order to that of the hairpin–Target, so that it forms a similar hairpin structure as the hairpin–Target with the same stability of the stem, however, because of the reversed sequence, the uncomplementary hairpin–Target should not hybridize with the F-D32-R.

The target molecules were incubated with the probe in the hybridization buffer at various molar ratios. Figure 5 shows a typical set of results of such experiments when the molar ratio of the probe to the target was kept at 1:5. When ss–Target was mixed with F-D32-R, the fluorescence intensity at 519 nm increased significantly (top spectrum in Fig. 5), indicating very limited FRET if any and the successful hybridization between ss–Target and F-D32-R, as depicted in the scheme in the lower left part of Figure 2b. This result was in agreement with the changes in FRET of a fluorescently double-labeled 15mer oligonucleotide that were reported by Parkhurst and Parkhurst (19). A small increase at 586.5 nm was also observed upon hybridization. This change cannot be ascribed to the increase in the fluorescence from the acceptor because the fluorescence spectra overlap each other; the decreased intensity at the peak wavelength of the acceptor would be buried under the considerably increased fluorescence of the donor. The possibility of the static quenching of the acceptor was tested by comparison of the excitation spectra of a DNA labeled with 6-carboxytetramethylrhodamine and of F-D32-R, because the static quenching should cause a change of the excitation spectrum (42). The resultant two spectra were nearly identical except that the spectrum of F-D32-R had a shoulder in the lower wavelength region due to the energy transfer (data not shown). This result indicated that the static quenching of 6-carboxytetramethylrhodamine did not take place.

In contrast to the results with the complementary ss–Target, no change in FRET occurred when the probe was incubated with the control DNA, D32, that had the same sequence as the probe (data not shown). We then examined whether the probe could interact with the ss–Target that had already formed a duplex with D32. D32 (150 pmol) and ss–Target (150 pmol) were mixed, heated at 85°C for 5 min and cooled slowly to room temperature, to assure complete formation of the duplex. Then F-D32-R (30 pmol) was added. The extent of the change in FRET was about half that observed with ss–Target (second spectrum from the top in Fig. 5). This result indicated that the probe could interact with ss–Target that had formed a duplex with D32 by displacing the D32 strand to a significant extent.

Incubation of the probe with hairpin–Target resulted in a smaller but still significant decrease in the extent of FRET. The increase in fluorescence at 519 nm was about one quarter of that with ss–Target (third spectrum from the top in Fig. 5). In this case, the FRET can be ascribed to competition between the intermolecular interaction with the probe and intramolecular formation of a stem. It is important to note here that part of the population of probe molecules hybridized to the complementary sequence that had formed the intramolecular double-stranded stem structure. It is of great interest that a thermodynamically favored intramolecular interaction could be partially displaced by a less favored intermolecular interaction. In contrast to the results with the hairpin–Target, no change in FRET was detected when the probe was incubated with the uncomplementary hairpin–Target (data not shown), that had no complementary sequence to the probe, indicating that the change in FRET observed with the hairpin–Target was not due to the non-specific interaction with the hairpin structure but due to the specific interaction between complementary sequences. This conclusion was confirmed by gel-shift assays (see below).

The difference between the results with hairpin–Target and duplex–Target can be ascribed to the higher stability of the product of the intramolecular hybridization as compared with the

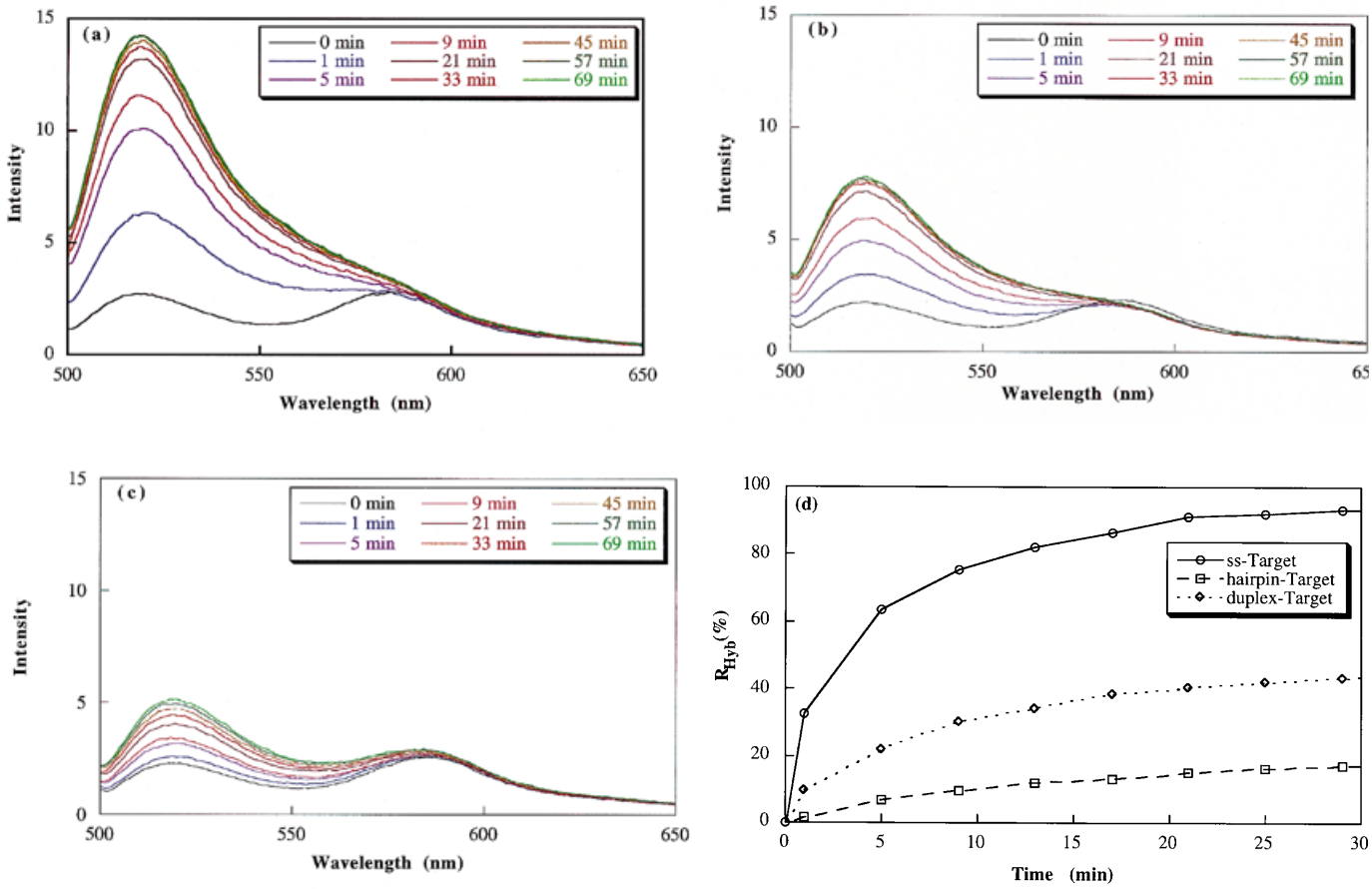

Figure 7. Time-dependence of changes in FRET. (**a**), (**b**), (**c**) Typical time-courses of changes in the fluorescence spectra of a 1 ml solution of probe (30 nM) after the addition of 150 pmol of ss–Target, of duplex–Target generated by mixing 150 pmol of ss–Target and the same amount of D32, and of 150 pmol of hairpin–Target, respectively. (**d**) The increase in the peak emission intensity (as a percentage) at 519 nm (denoted as R_{Hyb}) was employed as the measure of the extent of hybridization. Time-courses are shown for changes in R_{Hyb} at 30 min after the addition of either ss–Target (solid line), duplex–Target (dashed line) or hairpin–Target (broken line).

product of the intermolecular hybridization. These results indicate that the hybridization affinity of designed sequences, such as antisense molecules, can be estimated from measurements of FRET using fluorescently double-labeled antisense molecules and their target nucleic acids in solution.

To confirm that the change in FRET was due to the hybridization of the probe with target molecules, gel-shift assays were performed by using a fluorescence imaging analyzer. The probe was incubated with either ss–Target, D32, hairpin–Target, or uncomplementary hairpin–Target in various molar ratios, and electrophoresed with native polyacrylamide gel. Figure 6 shows the resultant signals of the fluorescence at 590 nm (red) and that at 530 nm (green) of the gel that had been excited with 488 nm blue laser beam. The incubation of the probe with ss–Target and hairpin–Target shifted the red original band on to the upper green band in dose-dependent manner. In contrast, the incubation with D32 or uncomplementary hairpin–Target did not show apparent shifts because they were unable to hybridize with the probe. These results demonstrate that the observed change in FRET was due to the hybridization with the targets because the change in FRET was accompanied with the increase in apparent molecular weights. The advantage of using fluorescently double-labeled oligonucleotides in gel-shift assays is that, in addition to the observations of shifted bands, they can be detected by different colors.

Time-dependent changes in FRET

The hybridization of the probe to its target molecule increases the peak intensity of emission at 519 nm (I_F). Therefore, the increase of the peak emission intensity in percentage at 519 nm (denoted as R_{Hyb}), estimated by the following equation, is a measure of the level of hybridization:

$$R_{Hyb} = (I_F - I_{F0})/(I_{F100} - I_{F0}) \times 100 \quad \mathbf{3}$$

where I_F is the intensity at 519 nm, I_{F0} is the I_F without any target molecules, and I_{F100} is the saturated value of I_F, where all probe molecules are hybridized to the target molecules. In this experiment, I_{F100} was the I_F obtained at the incubation of the probe with ss–Target (molar ratio was 1:5) for 70 min, where fluorescence had reached the maximum equilibrium value. We examined the time course of changes in R_{Hyb} after the addition of the probe to the hybridization solution that contained an appropriate target (Fig. 7). Measurements were made for up to 70 min (Fig. 7a–c). In the solution that contained ss–Target, the value of R_{Hyb} increased rapidly after mixing of the probe with ss–Target, and at 20 min after the mixing the rate of complex reached at 91% (Fig. 7a and d). By contrast, when the probe was incubated with either duplex–Target (Fig. 7b and d) or hairpin–Target (Fig. 7c and d), there was a more gradual increase and the

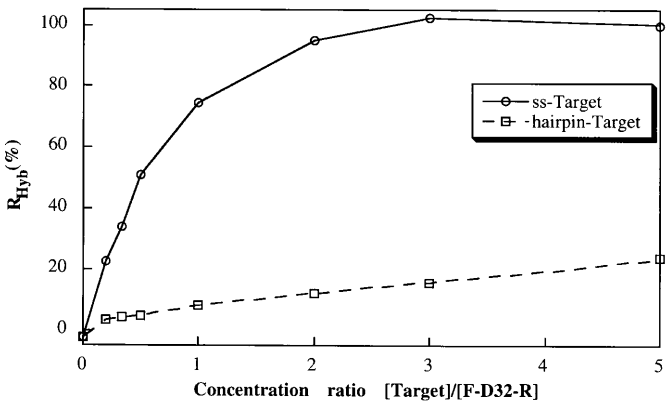

Figure 8. Dose-dependent changes in R_{Hyb}. Various amounts (0, 6, 10, 15, 30, 60, 90 and 150 pmol) of ss–Target (solid line) or hairpin–Target (broken line) were incubated with 30 pmol of F-D32-R for 70 min. The amount of the target strand apparently affected the extent of R_{Hyb} in a dose-dependent manner.

points at 70 min were ~48% and 24%, respectively, lower than that with the ss–Target/F-D32-R combination.

We next investigated the effect on the change in FRET of the molar ratio of the target to the probe (Fig. 8). The concentration of the probe was fixed at 30 nM. Concentrations of target DNAs were varied from 6 to 150 nM. Measurements were made at 70 min after the mixing of the probe with the target, in order to ensure that the hybridization reactions were complete (Fig. 7). The amount of target DNA apparently affected R_{Hyb} in a concentration-dependent manner. Figure 8 shows that 150 nM of ss–Target is enough to saturate 30 nM of F-D32-R, whereas 150 nM of hairpin–Target is not. The results presented in Figures 7 and 8 show that we were able successfully to distinguish the suitable target from the less accessible target at all ratios of target to probe that we examined.

Interactions between structured nucleic acids

Ribozymes are potential drugs for the treatment of genomic diseases (1,3,4,7). We investigated whether the present spectrofluorometric method might be useful for selecting the best sequence for a ribozyme (43), using our probe. As the first step toward this goal, the probe (F-D32-R) was designed on the basis of a hammerhead ribozyme; the RNA sequence was replaced by the corresponding DNA sequence because of facilitate synthesis and easier handling of DNA. In order to examine whether the probe with a higher-ordered structure could interact with a target embedded in a hairpin structure, we also synthesized six kinds of target DNA. Since the part of F-D32-R could form a hairpin structure that corresponded to the stem–loop II of the parental RNA ribozyme and since the sites for binding of F-D32-R to the target DNA were located at the 5′-end and the 3′-end, successful hybridization of F-D32-R with the linear target DNA should result in the complex depicted at the top of Figure 9a. In the case discussed above (Fig. 5), the hybridizing regions were as long as 32 nt. In the present case, the length of the hybridizing arms was 10 nt in total, as indicated by bold letters in Figure 4.

When F-D32-R was incubated with the linear target (D11–Target), the intensity at 519 nm (I_F) increased in a dose-dependent manner (Fig. 9b, inset), indicating that the extent of hybridization of the probe to the target was correlated with the concentration of the target. In the experiments for which results are shown in the inset in Figure 9b, the ratio of D11–Target to F-D32-R was changed by up to 100-fold, whereas the corresponding ratio for the ss–Target and F-D32-R was changed by only as much as 5-fold, for which results are shown in Figure 7. Despite such a high molar ratio of D11–Target to F-D32-R, the intensity at 519 nm (I_F) was lower than that observed for ss–Target and F-D32-R. This result was due to the shorter distance between the two fluorophores in the D11–Target/F-D32-R complex than that in the ss–Target/F-D32-R complex (compare the top scheme in Fig. 9a with the bottom left scheme in Fig. 2b) and also because the hybridization affinity of the D11–Target/F-D32-R complex should be lower than that of the ss–Target/F-D32-R complex. The lower affinity might be attributable to the fact that the annealing regions, consisting of two short five-base sequences, were separated at both termini of F-D32-R. The short terminal sequences might hybridize contiguously to the substrate oligonucleotide, skipping one base. This annealing pattern would closely resemble one with a mismatched nucleotide. Since a 15mer oligodeoxynucleotide has been reported to be unable to hybridize to targets with a mismatched base in the central site at 25°C (27), our probe might have had lower affinity for the D11–Target, requiring higher concentrations for hybridization. It should also be mentioned that, since the value of I_F did not reach a plateau in our experimental conditions, we could not estimate the exact extent of hybridization. Nevertheless, the experiments for which results are shown in the inset in Figure 9b clearly demonstrated that our strategy could be applied to identify the successful formation of a complex between a ribozyme and substrate-like molecules.

We examined the effect of the length of the stem that contained the target site for F-D32-R. Incubation of F-D32-R with various Stem-DNAs resulted in stem-length-dependent changes in FRET (Fig. 9b). The value of I_F with the Stem-12–Target was the same as with the D11–Target, indicating that the probe was successful in competition against the corresponding sequence within the intramolecular stem region. It is of great interest that the intermolecular hybridization between the target site of Stem-12–Target and F-D32-R was able to overcome the formation of the intramolecular stem within the Stem-12–Target, in particular, when we consider the stabilizing effect of the linkage tetranucleotides -GAAA- (44). By contrast, the probe failed to compete successfully with intramolecular interactions of oligonucleotides with stem structures of >14 bp, even when the Stem-DNA was present at molar ratios of target to probe of >100:1 (Fig. 9b).

We were able to distinguish successful hybridizations with structured nucleic acids from unsuccessful ones by following changes in FRET. These results suggest that this strategy should be applicable to the identification of the best target site for functional nucleic acids, including ribozymes and the more recently discovered DNA enzymes (45).

Origin of the decrease in FRET: measurements of anisotropy

The decrease in FRET can be explained most simply by an increase in the average distance between the donor and the acceptor upon hybridization. An increase in the intramolecular distance between the two fluorophores of the probe might occur upon hybridization as a consequence of the stiffness of the double-stranded oligonucleotide moiety within the probe. An alternative explanation is that inhibition of the dipole–dipole

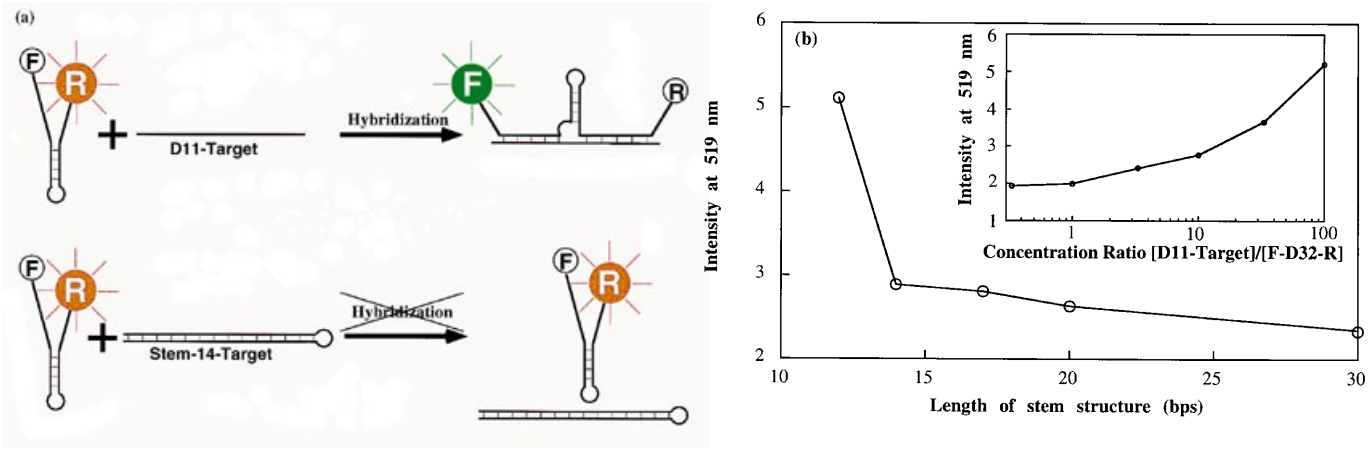

Figure 9. (**a**) Interaction of the hammerhead-ribozyme-shaped F-D32-R either with a linear target that mimicked a ribozyme substrate (D11–Target) or with a highly structured substrate (Stem-14–Target). When F-D32-R is mixed with D11–Target, FRET is expected to decrease as a result of hybridization. By contrast, the incubation with a stable stem–Target is not expected to lead to a decrease in FRET because of failure of hybridization. (**b**) Effects of the length of the duplex structure within the Stem–Target on the decrease in FRET. After a 70 min incubation of 30 pmol of F-D32-R with 3 nmol of stem–Target with various lengths, the intensity at 519 nm was measured. It was apparent that F-D32-R had hybridized to Stem-12–Target, but not to Stem–Targets with >14 bp in the stem. The inset shows the dose dependence of increase in the intensity at 519 nm after a 70 min incubation of 30 pmol of F-D32-R with D11–Target.

coupling of the FRET pair results from interference with rotation of the fluorophores. The rotational mobility of fluorophores can be estimated from steady-state fluorescence depolarization during the period between excitation and the emission of light, when the fluorophore is excited with polarized light (46,47). The extent of this phenomenon can be estimated from the fluorescence anisotropy (r), which can be calculated from equation **1** (see Materials and Methods). An increase in fluorescence anisotropy can be interpreted as evidence of a decrease in the rotational movement of fluorophores. To investigate these possibilities, we measured the fluorescence anisotropy of 6-carboxytetramethylrhodamine attached to the probe. The anisotropy was 0.31 ± 0.03 before hybridization. This value remained essentially constant throughout the 70 min incubation in a solution of the 32mer complementary ss–Target (r = 0.30 ± 0.02). The conservation of fluorescence anisotropy indicates that the rotational mobility of the fluorophore was consistently maintained during the hybridization. From these results, it appears that the decrease in FRET that accompanied hybridization was due to the spatial separation of the fluorophores that was associated with double-strand formation and not to their immobilization.

Titration of the ss–Target/F-D32-R by D32: demonstration of the similar affinity of the target (ss–Target) to the fluorescently double-labeled DNA (F-D32-R) and to the unmodified DNA (D32)

We investigated the possible difference in affinity of the target DNA (ss–Target) to the fluorescently double-labeled DNA (F-D32-R) and to the unmodified DNA (D32). This analysis was based on monitoring changes by a fluorescence imaging analyzer in the concentrations of shifted bands in a gel upon addition of the competitor molecules (titration). This gel-shift assay is similar to the one shown in Figure 6, however, in order to simplify the analysis, only the fluorescence at 530 nm (green) was monitored. Figure 10a shows a typical gel image obtained by the incubation of 200 nM of ss–Target and 200 nM of F-D32-R with various amounts of D32 following by native polyacrylamide gel electrophoresis. The amount

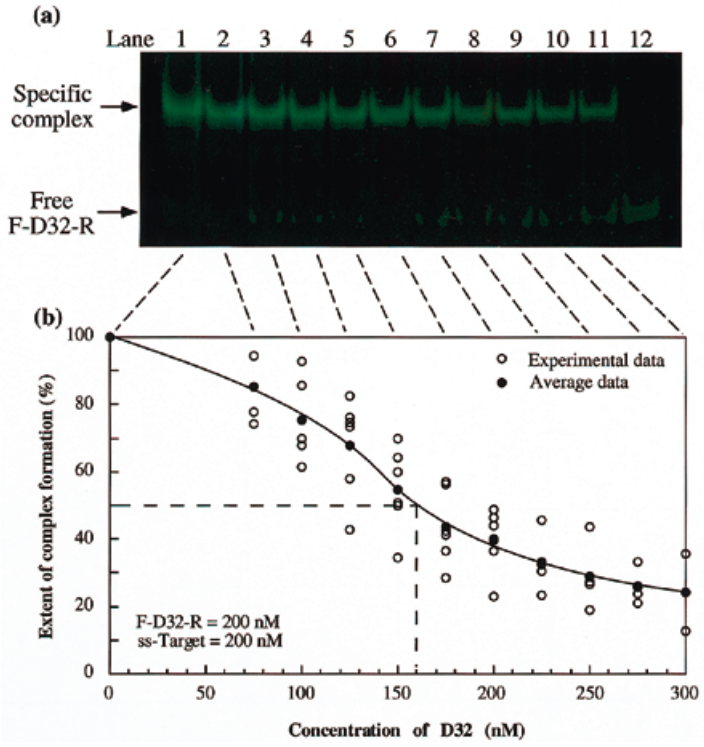

Figure 10. The difference in affinity of the target DNA (ss–Target) to the fluorescently double-labeled DNA (F-D32-R) or to the unmodified DNA (D32). (**a**) Various amounts of D32 were incubated overnight in the solution containing 200 nM of F-D32-R (2 pmol) and 200 nM of ss–Target. After the incubation, the mixtures were separated by a 12% native PAGE, analyzed and quantitated by a fluorscence imaging analyzer. Lanes 1–11 show results of the incubation with 0–300 nM of D32. Lane 12 is the control lane without D32 and ss–Target. (**b**) The extent of complex formation was estimated as described in the Materials and Methods. For 50% disruption of the bound complex of F-D32-R and ss–Target, <2 pmol of D32 was required, indicating that F-D32-R had a slightly lower affinity than did D32.

of F-D32-R bound to ss–Target decreased by the addition of D32 as shown in Figure 10. According to the titration curve shown in Figure 10b with the averaged experimental values, ~160 nM of D32 was required to replace the half of the F-D32-R bound to ss–Target (200 nM in total), indicating that F-D32-R had a little lower affinity to ss–Target than did D32. However, considering the experimental errors, the additions of the 6-carboxyfluorescein and 6-carboxy-tetramethylrhodamine to both ends of an oligonucleotide did not appear to significantly influence the stability of the duplex, a slightly lower affinity of the fluorescently double-labeled DNA to targets should enhance its specificity.

Conclusion

We have demonstrated here, for the first time, that fluorescently double-labeled oligonucleotides can be used to detect intermolecular interactions among structured nucleic acids, such as those with a hairpin structure, by measurements of changes in FRET. Thus, fluorescently double-labeled oligonucleotides should be useful as FRET probes in searches for suitable target sites embedded in highly ordered structures. In the case of molecular beacons (27), probes are dark when free in solution but they fluoresce brightly when hybridized to targets. In the case of our probes, the extent of FRET is maximal when probes are free in solution and a decrease in FRET indicates successful hybridization. Moreover, with our probes, monitoring of the integrity of oligonucleotides *in vitro* and, more importantly, *in vivo* is possible (22). Therefore, our probes should complement molecular beacons. The double-labeled oligonucleotides are also useful for the detection of specific complexes in gel-shift assays as demonstrated in Figure 6. Since the attached fluorophores might be expected to enhance the stability of oligonucleotides against exonucleases in cells, measurements of FRET using such oligonucleotide probes are also expected to be useful for identifying cells that express target genes and for monitoring gene expression *in vivo* continuously and in real time.

ACKNOWLEDGEMENTS

The authors thank Takeo Kohda of NIBH, Masayuki Masuko of Hamamatsu Photonics and Kaori Yasuda-Nakagawa of Molecular Dynamics for their helpful comments and Hideaki Shinshi of NIBH for letting us use the fluorescence imaging analyzer.

REFERENCES

1 Erickson,R.P. and Izant,J.G. (eds) (1992) In *Gene Regulation: Biology of Antisense RNA and DNA*. Raven Press, New York.
2 Murray,J.A.H. (ed.) (1992) In *Antisense RNA and DNA*. Wiley-Liss, New York.
3 Sarver,N., Cantin,E.M., Chang,P.S., Zaia,J.A., Ladne,P.A., Stephens,D.A. and Rossi,J.J. (1990) *Science* **247**, 1222–1225.
4 Ohkawa,J., Yuyama,N., Takebe,Y., Nishikawa,S. and Taira,K. (1993) *Proc. Natl. Acad. Sci. USA* **90**, 11302–11306.
5 Wagner,R.W. (1994) *Nature* **372**, 333–335.
6 Woolf,T.M., Melton,D.A. and Jennings,C.G.B. (1992) *Proc. Natl. Acad. Sci. USA* **89**, 7305–7309.
7 Eckstein,F. and Lilley,D.M. (eds) (1996) In *Catalytic RNA, Nucleic Acids and Molecular Biology, Vol. 10*. Springer-Verlag, Berlin, Heidelberg & New York.
8 Tomizawa,J.-I. (1984) *Cell* **38**, 861–870.
9 Polisky,B. (1988) *Cell* **55**, 929–932.
10 Stryer,L. (1978) *Annu. Rev. Biochem.* **47**, 819–846.
11 Herman,B. (1989) In Taylor,D.L. and Wang,Y. (eds) *Fluorescence Microscopy of Living Cells in Culture, Part B*. Academic Press, New York, pp. 220–245.
12 Tuschl,T., Gohlke,C., Jovin,T.M., Westhof,E. and Eckstein,F. (1994) *Science* **266**, 785–789.
13 Mergny,J.L., Boutorine,A.S., Garestier,T., Belloc,F., Rougee,M., Bulychev,N.V., Koshkin,A.A., Bourson,J., Lebedev,A.V., Valeur,B., Thuong,N.T. and Hélène,C. (1994) *Nucleic Acids Res.* **22**, 920–928.
14 Clegg,R.M., Murchie,A.I.H., Zechel,A. and Lilley,D.M.J. (1993) *Proc. Natl. Acad. Sci. USA* **90**, 2994–2998.
15 Jareserijman,E.A. and Jovin,T.M. (1996) *J. Mol. Biol.* **257**, 597–617.
16 Cooper,J.P. and Hagerman,P.J. (1990) *Biochemistry* **23**, 9261–9268.
17 Gohlke,C., Murchie,A.I. and Lilley,D.M.J. (1994) *Proc. Natl. Acad. Sci. USA* **91**, 11660–11664.
18 Sixou,S., Szoka,F.C.,Jr, Green,G.A., Giusti,B., Zon,G. and Chin,D.J. (1994) *Nucleic Acids Res.* **22**, 662–668.
19 Parkhurst,K.M. and Parkhurst,L.J. (1995) *Biochemistry* **34**, 285–292.
20 Bjornson,K.P., Amaratunga,M., Moore,K.J. and Lohman,T.M. (1994) *Biochemistry* **33**, 14306–14316.
21 Yang,M., Ghosh,S.S. and Millar,D.P. (1994) *Biochemistry* **33**, 15329–15337.
22 Uchiyama,H., Hirano,K., Kashiwasake-Jibu,M. and Taira,K. (1996) *J. Biol. Chem.* **271**, 380–384.
23 Ghosh,S.S., Eis,P.S., Blumeyer,K., Fearon,K. and Millar,D.P. (1994) *Nucleic Acids Res.* **22**, 3155–3159.
24 Lee,S.P., Censullo,M.L., Kim,H.G., Knutson,J.R. and Han,M.K. (1995) *Anal. Biochem.* **227**, 295–301.
25 Holland,P.M., Abramson,R.D., Watson,R. and Gelfand,D.H. (1991) *Proc. Natl. Acad. Sci. USA* **88**, 7276–7280.
26 Livak,K., Flood,S.J.A., Marmoro,J., Giusti,W. and Deetz,K. (1995) *PCR Methods Applic.* **4**, 357–362.
27 Tyagi,S. and Kramer,F.R. (1996) *Nature Biotechnol.* **14**, 303–308.
28 Ju,J., Glazer,A.N. and Mathies,R.A. (1996) *Nucleic Acids Res.* **24**, 1144–1148.
29 Hung,S.C., Ju,J., Mathies,R.A. and Glazer,A.N. (1996) *Anal. Biochem.* **238**, 165–170.
30 Zelphati,O. and Szoka,F.C. (1996) *Proc. Natl. Acad. Sci. USA* **93**, 11493–11498.
31 Beaucage,S.L. and Caruthers,M.H. (1981) *Tetrahedron Lett.* **22**, 1859–1861.
32 Nelson,P.S., Kent,M. and Muthini,S. (1992) *Nucleic Acids Res.* **20**, 6253–6259.
33 Mullah,B. Wyatt,P., Stevens,J. Andrus,A. and Livak,K. (1996) *Coll. Czech Chem. Comm.* **61**, 287.
34 Theisen,P., McCollum,C. and Andrus,A. (1992) *Nucleic Acids Symp. Ser.* **22**, 99–100.
35 Applied Biosystems (1993) US Patent #5 231 191 and patents pending.
36 Orita,M., Vinayak,R., Andrus,A., Warashina,M., Chiba,A., Kaniwa,H., Nishikawa,F., Nishikawa,S. and Taira,K. (1996) *J. Biol. Chem.* **271**, 9447–9454.
37 Zhou,D.-M., Usman,N., Wincott,F.E., Matulic-Adamic,J., Orita,M., Zhang,L.-H., Komiyama,M., Kumar,P.K.R. and Taira,K. (1996) *J. Am. Chem. Soc.* **118**, 5862–5866.
38 Zhou,D.-M., Kumar,P.K.R., Zhang,L.-H. and Taira,K. (1996) *J. Am. Chem. Soc.* **118**, 8969–8970.
39 Amontov,S. and Taira,K. (1996) *J. Am. Chem. Soc.* **118**, 1624–1628.
40 Zhou,D.-M., Zhang,L.-H. and Taira,K. (1997) *Proc. Natl. Acad. Sci. USA*, **94**, 14343–14348.
41 Warashina,M., Takagi,Y., Sawata,S., Zhou,D.-M., Kuwabara,T. and Taira,K. (1997) *J. Org. Chem.*, **62**, 9138–9147.
42 Lakowicz,J.R. (ed.) (1983) In *Principles of Fluorescence Spectroscopy*. Plenum Press, New York, pp. 264–271.
43 Fujita,S., Koguma,T., Ohkawa,J., Mori,K., Kohda,T., Kise,H., Nishikawa,S., Iwakura,M. and Taira,K. (1997) *Proc. Natl. Acad. Sci. USA* **94**, 391–396.
44 Hirao,I., Nishimura,Y., Naraoka,T., Watanabe,K., Arata,Y. and Miura,K. (1989) *Nucleic Acids Res.* **17**, 2223–2231.
45 Santro,S.W. and Joyce,G.F. (1997) *Proc. Natl. Acad. Sci. USA* **94**, 4262–4266.
46 Illsley,N.P., Lin,H.Y. and Verkman,A.S. (1987) *Biochemistry* **26**, 446–454.
47 Barcellona,M.L. and Gratton,E. (1996) *Biophys. J.* **70**, 2341–2351.